



## Enhancement of resonant and non-resonant magnetoelectric coupling in multiferroic laminates with anisotropic piezoelectric properties

Deepak Rajaram Patil, Yisheng Chai, Rahul C. Kambale, Byung-Gu Jeon, Kyongjun Yoo, Jungho Ryu, Woon-Ha Yoon, Dong-Soo Park, Dae-Yong Jeong, Sang-Goo Lee, Jeongho Lee, Joong-Hee Nam, Jeong-Ho Cho, Byung-Ik Kim, and Kee Hoon Kim

Citation: [Applied Physics Letters](#) **102**, 062909 (2013); doi: 10.1063/1.4792590

View online: <http://dx.doi.org/10.1063/1.4792590>

View Table of Contents: <http://scitation.aip.org/content/aip/journal/apl/102/6?ver=pdfcov>

Published by the [AIP Publishing](#)

---

### Articles you may be interested in

[The influence of low-level pre-stressing on resonant magnetoelectric coupling in Terfenol-D/PZT/Terfenol-D laminated composite structure](#)

J. Appl. Phys. **115**, 193906 (2014); 10.1063/1.4876721

[Multiferroism and enhancement of material properties across the morphotropic phase boundary of BiFeO<sub>3</sub>-PbTiO<sub>3</sub>](#)

J. Appl. Phys. **115**, 104104 (2014); 10.1063/1.4868319

[Magnetoelectric coupling in multiferroic laminated plates with giant magnetostrictive material layers](#)

J. Appl. Phys. **110**, 124514 (2011); 10.1063/1.3671400

[Giant sharp converse magnetoelectric effect from the combination of a piezoelectric transformer with a piezoelectric/magnetostrictive laminated composite](#)

Appl. Phys. Lett. **93**, 113503 (2008); 10.1063/1.2976329

[Multiferroic magnetoelectric composites: Historical perspective, status, and future directions](#)

J. Appl. Phys. **103**, 031101 (2008); 10.1063/1.2836410

---

The image shows the cover of an Applied Physics Reviews journal. It features a blue and orange color scheme with a molecular structure background. The text 'NEW Special Topic Sections' is prominently displayed in white. Below it, 'NOW ONLINE' is written in yellow, followed by the title 'Lithium Niobate Properties and Applications: Reviews of Emerging Trends' in white. The AIP Applied Physics Reviews logo is in the bottom right corner.

**NEW Special Topic Sections**

**NOW ONLINE**  
Lithium Niobate Properties and Applications:  
Reviews of Emerging Trends

**AIP** Applied Physics Reviews

# Enhancement of resonant and non-resonant magnetoelectric coupling in multiferroic laminates with anisotropic piezoelectric properties

Deepak Rajaram Patil,<sup>1,a)</sup> Yisheng Chai,<sup>1,a)</sup> Rahul C. Kambale,<sup>2</sup> Byung-Gu Jeon,<sup>1</sup> Kyongjun Yoo,<sup>1</sup> Jungho Ryu,<sup>2,b)</sup> Woon-Ha Yoon,<sup>2</sup> Dong-Soo Park,<sup>2</sup> Dae-Yong Jeong,<sup>3</sup> Sang-Goo Lee,<sup>4</sup> Jeongho Lee,<sup>4</sup> Joong-Hee Nam,<sup>5</sup> Jeong-Ho Cho,<sup>5</sup> Byung-Ik Kim,<sup>5</sup> and Kee Hoon Kim<sup>1,b)</sup>

<sup>1</sup>CeNSCMR, Department of Physics and Astronomy, Seoul National University, Seoul 151-747, Korea

<sup>2</sup>Functional Ceramics Group, Korea Institute of Materials Science (KIMS), 66 Sangnam-Dong, Changwon, Gyeongnam 641-831, Korea

<sup>3</sup>School of Materials Engineering, Inha University, Incheon 402-751, Korea

<sup>4</sup>iBULe Photonics Co. Ltd, 7-39 Songdo-dong Yeonsu-gu Incheon, Korea

<sup>5</sup>Center for Electronic Component Research, Korea Institute of Ceramic Engineering and Technology, Seoul 153-801, Korea

(Received 29 November 2012; accepted 4 February 2013; published online 15 February 2013)

Giant transverse magnetoelectric voltage coefficients  $|\tilde{\alpha}_E| = 751$  and  $305$  V/cmOe at two electromechanical antiresonance frequencies are found in the symmetric metglas/[011]-oriented  $0.7\text{Pb}(\text{Mg}_{1/3}\text{Nb}_{2/3})\text{O}_3\text{-}0.3\text{PbTiO}_3$  crystal/metglas laminate. Unique torsional and diagonal vibration modes are identified to be responsible for those giant  $|\tilde{\alpha}_E|$  values. Moreover,  $\tilde{\alpha}_E$  is found to be anisotropic depending on the in-plane magnetic field directions, making the piezoelectrics with anisotropic planar piezoelectricity potentially useful base materials for multi-frequency, phase-sensitive magnetoelectric devices. © 2013 American Institute of Physics.  
[\[http://dx.doi.org/10.1063/1.4792590\]](http://dx.doi.org/10.1063/1.4792590)

The magnetoelectric (ME) effect,<sup>1</sup> induction of either electric polarization ( $P$ ) by a magnetic field ( $H$ ) or magnetization ( $M$ ) by an electric field ( $E$ ), holds great potential for many device applications such as energy harvesters,<sup>2</sup> field sensors,<sup>3</sup> gyrators,<sup>4</sup> and transducers.<sup>5</sup> Toward this end, multiferroic composites, wherein magnetostrictive and piezoelectric phases generate a sizable ME effect via strain coupling, have been extensively studied both theoretically<sup>6-8</sup> and experimentally,<sup>9-12</sup> for they exhibit a much higher ME voltage coefficient  $\alpha_E = \delta E / \delta H$  at room temperature than single-phase counterparts. To improve the ME voltage response, researchers have tried to use numerous material combinations with superior striction properties or better interface coupling by using, e.g., different connectivity schemes such as 0-3 type particulates, 2-2 type laminates, 1-3 type fiber or rod composites, and 1-2 type fiber laminates.<sup>9-12</sup>

Based on the extensive research, the current highest ME voltage coefficient is realized in the 1-2 structure using a three phase composite made of  $\text{Pb}(\text{Zr,Ti})\text{O}_3$  ceramic fibers/phosphor copper-sheet and  $\text{NdFeB}$  magnets, giving rise to  $\sim 16\,000$  V/cmOe at a bending resonance.<sup>13</sup> However, such 1-2 composites generally require much longer sample length ( $\sim 100$  mm) than 2-2 type laminates (mostly  $< 30$  mm) and more difficult fabrication methods.<sup>13</sup> In this sense, the symmetric 2-2 laminates, in which a piezoelectric layer is sandwiched by two magnetostrictive layers, have been more commonly adopted and is likely to be more feasible in real applications. Moreover, among the various 2-2 laminates, the combination of the metglas and  $x\text{Pb}(\text{Mg}_{1/3}\text{Nb}_{2/3})\text{O}_3\text{-}(1-x)\text{PbTiO}_3$  (PMN-PT) or related piezoelectric materials

has been most popular in recent years, because of their superior ME sensitivity.<sup>14-16</sup> For instance, the highest  $\alpha_E$  of 448 V/cmOe observed at resonance in a laminate combined with metglas and  $0.05\text{Pb}(\text{Mn}_{1/3}\text{Sb}_{2/3})\text{O}_3\text{-}0.95(\text{Pb,Zr})\text{TiO}_3$  is still comparable to that of the 1-2 structure.<sup>17</sup> Based on this previous research, it is the purpose of the present work to tailor the ME coupling further in the laminate structure. This is a technically important as well as fundamentally interesting goal.

We note that until now, almost all the studies on the ME coupling of symmetric 2-2 laminates have adopted the magnetostrictive and piezoelectric phases having isotropic in-plane striction properties except limited cases on converse ME effects.<sup>14,18,19</sup> For instance, most researchers have used single crystals of PMN-PT or related piezoelectrics, which are cut to make its plane vector parallel to the [001]-direction (Fig. 1(a), cut-A). Because PMN-PT has a rhombohedral structure and eight possible polarization directions along the pseudocubic [111] directions, an electrical poling along the [001]-direction will then generate a multidomain state with four dipole orientations, giving rise to an isotropic piezoelectric response in the plane (i.e., transverse piezoelectric coefficients  $d_{31} = d_{32} = -921$  pC/N,<sup>20</sup> meaning that the voltage generated along the 3-axis per unit force applied either along the 1- or 2-axes is the same).<sup>21</sup> Once this isotropic piezoelectric material is combined with the magnetostrictive phase to form a laminate structure, the resultant ME response is supposed to be limited, due to the opposite signs in the in-plane magnetostrictions under in-plane magnetic fields (i.e.,  $q_{11} \approx -2q_{12}$  is satisfied between in-plane piezomagnetic coefficients  $q_{11}$  and  $q_{12}$ ).<sup>22</sup> In contrast, if the PMN-PT crystal is cut such that the plane vector becomes parallel to [011]-direction (Fig. 1(b), cut-B), two dipole orientations are allowed to result in anisotropic piezoelectric coefficients (e.g.,  $d_{31} = 610$

<sup>a)</sup>D. R. Patil and Y. S. Chai contributed equally to this work.

<sup>b)</sup>Authors to whom correspondence should be addressed. Electronic addresses: jhryu@kims.re.kr and khkim@phya.snu.ac.kr.

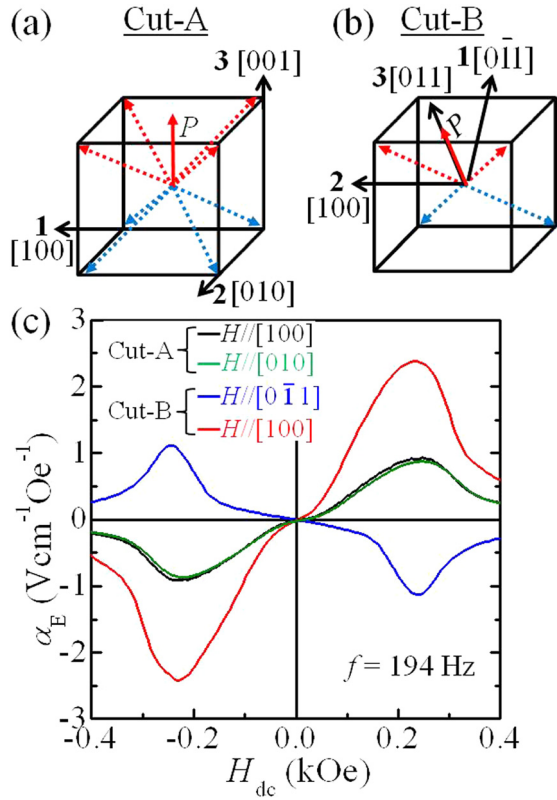


FIG. 1. Schematic of PMN-PT single crystals with (a) [001]-orientation (cut-A) and (b) [011]-orientation (cut-B), respectively. Out of 8 possible polarization directions inherent to the rhombohedral symmetry, 4 (2) polarization directions are chosen for cut-A (cut-B) upon poling (red dotted lines). (c)  $H_{dc}$  dependence of  $\alpha_E$  at a frequency  $f=194$  Hz for metglas/PMN-PT/metglas laminates with different PMN-PT orientations.

and  $d_{32} = -1883$  pC/N,<sup>23</sup> which are superior to those of isotropic ones.<sup>21,24</sup> Consequently, in the laminate using the cut-B type crystal, one can expect an enhancement in the resultant ME coupling as a result of the strong anisotropy in the transverse piezoelectric properties.

In this letter, we present systematic investigations on the ME coupling in a symmetric 2-2 laminate having a representative piezoelectric crystal (PMN-PT) particularly with anisotropic transverse piezoelectric coefficients. With this approach, we obtained a record-high, resonant ME voltage coefficient of  $\sim 751$  V/cmOe among the 2-2 laminates. Moreover, we identified unique torsional and diagonal vibration modes as being responsible for the greatly enhanced ME voltage coefficients at two main frequencies.

High quality PMN-PT ( $0.7\text{Pb}(\text{Mg}_{1/3}\text{Nb}_{2/3})\text{O}_3-0.3\text{PbTiO}_3$ ) single crystals were grown by the Bridgeman method (IBULE Photonics, Korea) and cut in a planar shape with a thickness of 0.3 mm. The ME laminates were prepared by stacking six metglas layers (2605SA1, Metglas Inc., USA) of thickness 0.025 mm on the top and bottom surfaces of the PMN-PT using a silver epoxy. The samples were poled by applying a dc electric field of 10 kV/cm. To investigate quantitatively the ME coupling, a magnetolectric susceptometer, working at both resonant and low frequency conditions, was used. A pair of Helmholtz coils were used to generate AC magnetic field  $\delta H_{ac}$  in a broad frequency range ( $f=194$  Hz–1 MHz) and the resultant AC voltage across the sample was measured by a

lock-in amplifier as a function of  $H_{dc}$  to estimate a complex ME voltage coefficient  $\tilde{\alpha}_E \equiv \alpha_E + i\text{Im}(\tilde{\alpha}_E)$ . Impedance spectra were measured by an impedance analyzer (HP4194A, USA). The in-plane vibrational displacements were measured by a laser Doppler vibrometer (Polytec, Germany) under the sinusoidal transverse electric fields. The analyses of vibrational modes were performed by the ATILA program, which performs calculations based on a finite-element method.

To investigate the effects of the different PMN-PT orientations on the ME response, we prepared two types of symmetric metglas/PMN-PT/metglas laminates with lateral dimensions of  $10 \times 10$  mm<sup>2</sup> using the cut-A and cut-B single crystals of PMN-PT. Figure 1(c) presents  $\alpha_E$  curves of the laminate with cut-A crystal measured at  $f=194$  Hz for  $H_{dc} // [100]$  and  $// [010]$ . For both  $H_{dc}$  directions,  $\alpha_E$  exhibits a typical  $H_{dc}$  dependence showing a sign change with respect to the reversal of  $H_{dc}$  direction. Moreover, the  $\alpha_E$  curves are almost identical in both directions. In the 2-2 laminates with an isotropic piezoelectric properties, the ME voltage coefficient  $\alpha_{E31}$ , referring to the transverse electric field generated along the 3-axis under  $H // 1$ -axis can be calculated through the following relation:<sup>8</sup>

$$\alpha_{E31} = -\frac{kf(1-f)d_{31}(q_{11} + q_{21})}{\epsilon_{33}s_{11} - 2kfd_{31}^2}, \quad (1)$$

where  $s_{11} = f(s_{11}^p + s_{12}^p) + k(1-f)(s_{11}^m + s_{12}^m)$ . Here,  $f$  is the volume fraction of the magnetic phase,  $\epsilon_{33}$  is the dielectric permittivity of the piezoelectric phase,  $s_{ij}^{p(m)}$  are piezoelectric (magnetic) compliances,  $k$  is the interface coupling parameter ( $k=1$  for an ideal interface and  $k=0$  for the case without friction),  $d_{ij}$  are the transverse piezoelectric coefficients, and  $q_{ij}$  are the piezomagnetic coefficients, i.e.,  $q_{ij} = d\lambda_{ij}/dH_j$ , where  $\lambda_{ij}$  is the magnetostriction

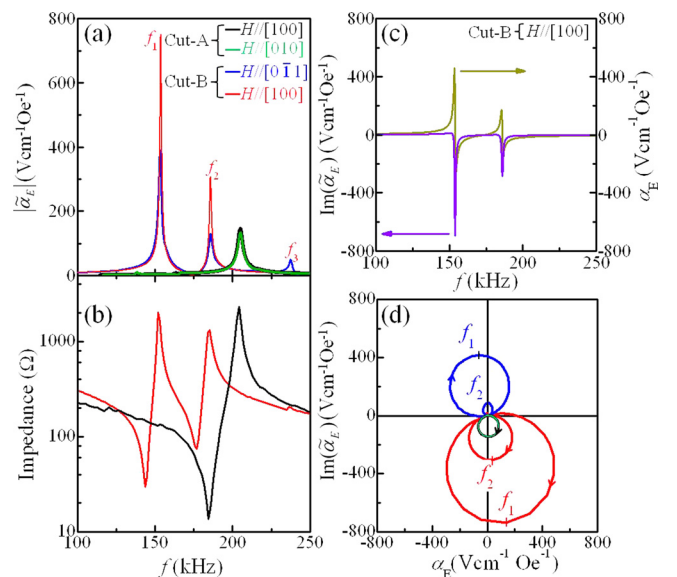


FIG. 2. Frequency dependence of (a) the modulus of complex ME voltage coefficient, i.e.,  $|\tilde{\alpha}_E|$  along different  $H$  directions and of (b) impedance for the ME laminates. (c) Frequency dependence of  $\alpha_E$  and  $\text{Im}(\tilde{\alpha}_E)$  along  $H // [100]$  for the laminate with cut-B PMN-PT. (d) Cole-cole plots for data in (a). The arrows indicate the frequency increasing direction. All the measurements were performed at  $H_{dc} = 240$  Oe.

( $i, j = 1$  and  $2$ ). Note that  $\alpha_{E31} = \alpha_{E32}$  holds for the isotropic piezoelectric/magnetostrictive media as the equality relations of  $d_{31} = d_{32}$ ,  $q_{11} = q_{22}$ , and  $q_{12} = q_{21}$  are valid, evidently explaining the isotropic behavior observed in the laminate with cut-A crystal.

In sharp contrast, the laminate with the cut-B crystal shows strongly anisotropic behavior:  $\alpha_E$  values along  $H//[0\bar{1}1]$  and  $H//[100]$  clearly show opposite signs and the maximum magnitudes become 1.12 and 2.49 V/cmOe, respectively, constituting their ratio of  $\sim 0.45$ . It is also noteworthy

that the maximum value of 2.49 V/cmOe is about 2.7 times larger than that of the isotropic laminate (0.91 V/cmOe). The anisotropy in the transverse ME voltage coefficients is likely due to the cut-B single crystal with a positive  $d_{31}$  and a negative  $d_{32}$ . We could indeed deduce new sets of formula for the ME signal in the laminate with anisotropic piezoelectric properties based on the fundamental constitutive equations in a recent theoretical study,<sup>25</sup> in which the transverse ME coefficients,  $\alpha_{E31} = \delta E_3 / \delta H_1$  ( $H//[0\bar{1}1]$ ), and  $\alpha_{E32} = \delta E_3 / \delta H_2$  ( $H//[100]$ ) are predicted as

$$\alpha_{E31} = \frac{(d_{31}s_{22}q_{11} + d_{32}s_{11}q_{12}) - s_{21}(d_{31}q_{12} + d_{32}q_{11})}{2\varepsilon_{33}^p[s_{11}s_{22} - (s_{21})^2] - [s_{22}(d_{31})^2 + s_{11}(d_{32})^2 - 2s_{21}d_{31}d_{32}]} \quad (2)$$

and

$$\alpha_{E32} = \frac{(d_{31}s_{22}q_{21} + d_{32}s_{11}q_{22}) - s_{21}(d_{31}q_{22} + d_{32}q_{21})}{2\varepsilon_{33}^p[s_{11}s_{22} - (s_{21})^2] - [s_{22}(d_{31})^2 + s_{11}(d_{32})^2 - 2s_{21}d_{31}d_{32}]} \quad (3)$$

where  $s_{22} = \frac{(s_{22}^p + s_{22}^m)}{2}$ ,  $s_{21} = \frac{(s_{21}^p + s_{21}^m)}{2}$ ,  $s_{11} = \frac{(s_{11}^p + s_{11}^m)}{2}$ , and  $s_{12} = \frac{(s_{12}^p + s_{12}^m)}{2}$ . Note that Eq. (2) is easily converted to Eq. (1) once the isotropic transverse piezoelectric property is assumed, i.e.,  $s_{11}^p = s_{22}^p$ ,  $s_{12}^p = s_{21}^p$ , and  $d_{31}^p = d_{32}^p$ . Upon applying the conditions of the interface coupling constant  $k = 1$ , the volume fraction of magnetostrictive phase  $f = 0.5$ , and the reported parameters<sup>22,26</sup> into Eqs. (2) and (3), we find that the signs and magnitudes of  $\alpha_{E31}$  and  $\alpha_{E32}$  are clearly different and the calculated ratio between the maxima of  $\alpha_{E31}$  and  $\alpha_{E32}$  is  $\sim 0.57$ , being roughly consistent with the experimental observation. Therefore, we conclude that the anisotropic ME response is a consequence of the anisotropic transverse piezoelectric properties ( $d_{31} \neq d_{32}$  and  $s_{11}^p \neq s_{22}^p$ ).

The anisotropic ME response can also be revealed in resonant conditions. For comparison, we first measured the frequency dependence of  $|\tilde{\alpha}_E|$  for the laminate with cut-A PMN-PT, finding only one single peak at a frequency of  $f = 205$  kHz (Fig. 2(a)). Similar to the low frequency data, there is almost no difference in the  $|\tilde{\alpha}_E|$  curves measured for the two in-plane  $H$  directions. In addition, it is confirmed that the peak frequency occurs at the maximum in the impedance data (Fig. 2(b)), which corresponds to the electromechanical antiresonance of the piezoelectric layer as previously proved by Cho and Priya.<sup>17</sup> In the case of the laminate with cut-B crystal, two strong  $|\tilde{\alpha}_E|$  peaks at  $f_1 = 154$  kHz and  $f_2 = 186$  kHz and one weak peak at  $f_3 = 238$  kHz were observed for both  $H//[0\bar{1}1]$  and  $[100]$ . The  $|\tilde{\alpha}_E|$  peaks are also located at the antiresonance points as demonstrated in the impedance data. Moreover, the magnitude of each  $|\tilde{\alpha}_E|$  peak is different for the two  $H$  directions: for  $H//[100]$ ,  $|\tilde{\alpha}_E| = 751$  V/cmOe at  $f_1$  and 305 V/cmOe at  $f_2$ , while they are 391 V/cmOe and 128 V/cmOe for  $H//[0\bar{1}1]$ . It should be stressed that the  $|\tilde{\alpha}_E| = 751$  V/cmOe is a record-high value for symmetric 2-2 type laminates<sup>12</sup> and is enhanced by about five times over the isotropic laminate (147 V/cmOe).

The anisotropic piezoelectric property not only induces at least two maxima of  $\tilde{\alpha}_E$  with anisotropy in their magnitude but also results in different phases for different  $H$  orientations. Since  $\tilde{\alpha}_E$  is a complex quantity, the real and imaginary components of  $\tilde{\alpha}_E$  generally exhibit characteristic frequency dependence as shown in Fig. 2(c). For  $H//[100]$ , the imaginary component  $\text{Im}(\tilde{\alpha}_E)$  is almost zero, while  $\alpha_E$  maintains a small positive value at lower frequencies. When the frequency is increased to pass the antiresonant frequency,  $\text{Im}(\tilde{\alpha}_E)$  mainly shows a dip, while  $\alpha_E$  shows a positive peak and a negative dip structure successively. In contrast, the phase of  $\tilde{\alpha}_E$  changed by  $180^\circ$  for  $H//[0\bar{1}1]$ . Namely,  $\text{Im}(\tilde{\alpha}_E)$

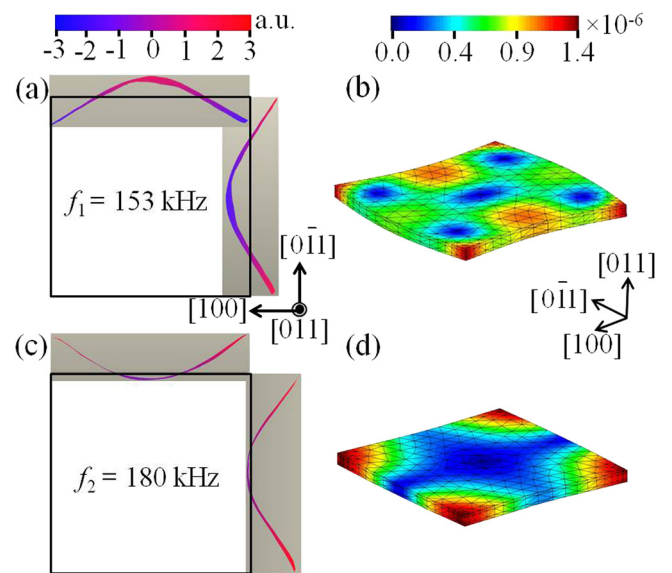


FIG. 3. The maximum displacement as measured by laser Doppler vibrometry at antiresonant frequencies (a)  $f_1 = 153$  kHz and (c)  $f_2 = 180$  kHz for the laminate with cut B PMN-PT. Simulated displacement amplitude patterns are represented at the corresponding vibrational modes at (b)  $f_1 = 153$  kHz and (d)  $f_2 = 180$  kHz.

mainly had a peak, while  $\alpha_E$  showed successively a negative dip and a positive peak structure. This contrasting behavior is demonstrated in the Cole-Cole plot in Fig. 2(d), displaying the  $\text{Im}(\tilde{\alpha}_E)$  versus  $\alpha_E$  curves with frequency up to 250 kHz. The circles for  $H//[0\bar{1}1]$  and  $H//[100]$  occupy clearly the opposite positions in the plot, showing that the phase of  $\tilde{\alpha}_E$  is different by  $180^\circ$ . In the isotropic laminate with cut-A crystal, however, there was no difference in the phase and magnitude of  $\tilde{\alpha}_E$  for the two  $H$  directions, consistent with the previous report.<sup>27</sup> Our results thus demonstrate that the phase of the resonant  $\tilde{\alpha}_E$  can be determined by the  $H$  direction in the ME laminate with anisotropic transverse piezoelectricity. It is worthwhile to mention that the current experimental findings on the resonant conditions showing at least two resonance frequencies and phase difference with each other are also consistent with the recent theory.<sup>25</sup>

To better understand the origin of unique resonant ME signals in the anisotropic laminate, we have investigated the corresponding vibrational modes. Figure 3(a) illustrates the maximum edge displacements along  $[0\bar{1}1]$  and  $[100]$  directions at  $f_1 = 153$  kHz as measured by the laser Doppler vibrometer. The vibrations at the corners and at the centers have similar magnitudes with opposite displacements along both directions. However, we could not determine the relative phase between the displacements along the  $[0\bar{1}1]$  and  $[100]$  directions, as the measurements were performed separately for both directions. On the other hand, the vibrational mode simulation by the ATILA program suggests an asymmetric torsional mode (Fig. 3(b)). In this mode, the curvature of the displacements along  $[0\bar{1}1]$  and  $[100]$  directions is quite similar to our experimental data (Fig. 3(a)) although those displacements are out of phase with each other. Therefore, it is quite likely that the vibration mode at  $f_1$  is indeed a torsional type. For the vibration mode at  $f_2 = 180$  kHz, the maximum displacements are observed at the corners and the centers are almost fixed for  $[0\bar{1}1]$  and  $[100]$  directions (Fig. 3(c)). The resultant curvatures are very similar to the mode simulation result, in which an asymmetric diagonal vibration mode is predicted (Fig. 3(d)). In this case, the displacements along the two orthogonal directions are in-phase with each other. In addition, the third ME peak is found to have a combination of face extensional and diagonal modes, and for the laminate with cut-A PMN-PT, a face extensional mode could be identified.

Finally, the giant  $|\tilde{\alpha}_E|$  values seem to be consistent with the vibration behavior in those modes. When the  $|\tilde{\alpha}_E|$  peaks at the antiresonant frequencies, the impedance is maximized and thus the capacitance and dielectric constant are minimized.<sup>17</sup> The smaller the dielectric constant, the smaller the averaged charge that can then be induced by a fixed electric field in PMN-PT. Conversely, a charge induced to PMN-PT by the strain coupling can most effectively generate an electric voltage in the vibrational mode. The torsional and diagonal modes having a small net displacement is likely to induce small net surface charge by an electric field, leading to a small capacitance. Therefore, it is expected to result in the largest, direct ME signal, consistent with our observation.

In conclusion, we demonstrate giant ME voltage coefficients and magnetic-field-direction dependent ME signals at both low and resonance frequencies in the symmetric ME laminate having the PMN-PT crystal with anisotropic transverse piezoelectric coefficients. The torsional and diagonal vibration modes are identified to result in the giant ME voltage coefficients at antiresonant conditions, which can be applicable to multi-frequency, phase-sensitive ME devices. Our experimental results also imply that any ME laminates or thin ME films with the piezoelectrics with anisotropic piezoelectric coefficients can show a similar type of enhancement in the ME coupling.

We appreciate critical readings/comments on the manuscript from G. R. Stewart. This work was financially supported by the National CRI funding (2010-0018300) and Fundamental R&D Program for Core Technology of Materials. Work at KIMS was supported by NRF grant by MEST (2012R1A1A2A10041947) and the Converging Research Center Program funded by the MEST (2012K001435).

- <sup>1</sup>N. A. Spaldin and M. Fiebig, *Science* **309**, 391 (2005).
- <sup>2</sup>P. Li, Y. Wen, P. Liu, X. Li, and C. Jia, *Sens. Actuators A* **157**, 100 (2010).
- <sup>3</sup>Y. K. Fetisov, A. A. Bush, K. E. Kamentsev, A. Y. Ostashchenko, and G. Srinivasan, *IEEE Sens. J.* **6**, 935 (2006).
- <sup>4</sup>S. X. Dong, J. Y. Zhai, J. F. Li, D. Viehland, and M. I. Bichurin, *Appl. Phys. Lett.* **89**, 243512 (2006).
- <sup>5</sup>S. X. Dong, J. F. Li, and D. Viehland, *Appl. Phys. Lett.* **83**, 2265 (2003).
- <sup>6</sup>G. Harshe, J. O. Dougherty, and R. E. Newnham, *Int. J. Appl. Electro-magn. Mater.* **4**, 145 (1993).
- <sup>7</sup>M. I. Bichurin, V. M. Petrov, and G. Srinivasan, *J. Appl. Phys.* **92**, 7681 (2002).
- <sup>8</sup>M. I. Bichurin, V. M. Petrov, S. V. Averkin, and A. V. Filippov, *Phys. Solid State* **52**, 2116 (2010).
- <sup>9</sup>S. Priya, R. Islam, S. Dong, and D. Viehland, *J. Electroceram.* **19**, 147 (2007).
- <sup>10</sup>C. W. Nan, M. I. Bichurin, S. X. Dong, D. Viehland, and G. Srinivasan, *J. Appl. Phys.* **103**, 031101 (2008).
- <sup>11</sup>J. Ma, J. Hu, Z. Li, and C. W. Nan, *Adv. Mater.* **23**, 1062 (2011).
- <sup>12</sup>G. Srinivasan, *Annu. Rev. Mater. Res.* **40**, 153 (2010).
- <sup>13</sup>G. Liu, X. Li, J. Chen, H. Shi, W. Xiao, and S. Dong, *Appl. Phys. Lett.* **101**, 142904 (2012).
- <sup>14</sup>Y. Chen, A. L. Geiler, T. Fitchorov, C. Vittoria, and V. G. Harris, *Appl. Phys. Lett.* **95**, 182501 (2009).
- <sup>15</sup>C.-S. Park, K.-H. Cho, M. A. Arat, J. Evey, and S. Priya, *J. Appl. Phys.* **107**, 094109 (2010).
- <sup>16</sup>R. C. Kambale, D.-Y. Jeong, and J. Ryu, *Adv. Condens. Matter Phys.* **2012**, 1.
- <sup>17</sup>K. H. Cho and S. Priya, *Appl. Phys. Lett.* **98**, 232904 (2011).
- <sup>18</sup>J. Lou, D. Reed, C. Pettiford, M. Liu, P. Han, S. Dong, and N. X. Sun, *Appl. Phys. Lett.* **92**, 262502 (2008).
- <sup>19</sup>M. Liu, O. Obi, J. Lou, Y. Chen, Z. Cai, S. Stoute, M. Espanol, M. Lew, X. Situ, K. S. Ziemer, V. G. Harris, and N. X. Sun, *Adv. Funct. Mater.* **19**, 1826 (2009).
- <sup>20</sup>H. Cao, V. H. Schmidt, R. Zhang, W. Cao, and H. Luo, *J. Appl. Phys.* **96**, 549 (2004).
- <sup>21</sup>S. Zhang, N. P. Sherlock, R. J. Meyer, and T. R. Shrout, *Appl. Phys. Lett.* **94**, 162906 (2009).
- <sup>22</sup>D. Patil, J. H. Kim, Y. S. Chai, J. H. Nam, J. H. Cho, B. I. Kim, and K. H. Kim, *Appl. Phys. Express* **4**, 073001 (2011).
- <sup>23</sup>P. F. Wang, L. Luo, D. Zhou, X. Zhao, and H. Luo, *Appl. Phys. Lett.* **90**, 212903 (2007).
- <sup>24</sup>T. Wu, P. Zhao, M. Bao, A. Bur, J. L. Hockel, K. Wong, K. P. Mohanchandra, C. S. Lynch, and G. P. Carman, *J. Appl. Phys.* **109**, 124101 (2011).
- <sup>25</sup>D. R. Patil *et al.*, e-print [arXiv:1211.7003](https://arxiv.org/abs/1211.7003).
- <sup>26</sup>J. Zhai, S. Dong, Z. Xing, J. Li, and D. Viehland, *Appl. Phys. Lett.* **89**, 083507 (2006).
- <sup>27</sup>J. Zhai, J. Li, D. Viehland, and M. I. Bichurin, *J. Appl. Phys.* **101**, 014102 (2007).